



UNIVERSITY OF LEEDS

This is a repository copy of *Intra-annual oxygen isotopes in the tree rings record precipitation extremes and water reservoir levels in the Metropolitan Area of São Paulo, Brazil*.

White Rose Research Online URL for this paper:
<https://eprints.whiterose.ac.uk/163243/>

Version: Accepted Version

Article:

Locosselli, GM, Brienen, R orcid.org/0000-0002-5397-5755, de Souza Martins, VT et al. (5 more authors) (2020) Intra-annual oxygen isotopes in the tree rings record precipitation extremes and water reservoir levels in the Metropolitan Area of São Paulo, Brazil. *Science of The Total Environment*. 140798. ISSN 0048-9697

<https://doi.org/10.1016/j.scitotenv.2020.140798>

© 2020 Elsevier B.V. Licensed under the Creative Commons Attribution-NonCommercial-NoDerivatives 4.0 International License (<http://creativecommons.org/licenses/by-nc-nd/4.0/>).

Reuse

This article is distributed under the terms of the Creative Commons Attribution-NonCommercial-NoDerivatives (CC BY-NC-ND) licence. This licence only allows you to download this work and share it with others as long as you credit the authors, but you can't change the article in any way or use it commercially. More information and the full terms of the licence here: <https://creativecommons.org/licenses/>

Takedown

If you consider content in White Rose Research Online to be in breach of UK law, please notify us by emailing eprints@whiterose.ac.uk including the URL of the record and the reason for the withdrawal request.



eprints@whiterose.ac.uk
<https://eprints.whiterose.ac.uk/>

1 **Intra-annual oxygen isotopes in the tree rings record precipitation extremes and**
2 **water reservoir levels in the Metropolitan Area of São Paulo, Brazil**

3

4 Giuliano Maselli Locosselli^{1,2*}, Roel Brienen³, Veridiana Teixeira de Souza Martins⁴,
5 Emanuel Gloor³, Arnoud Boom⁵, Evelyn Pereira de Souza¹, Paulo Hilário Nascimento
6 Saldiva², Marcos Silveira Buckeridge^{1,2}

7

8 ¹Instituto de Biociências, Universidade de São Paulo, São Paulo, Brazil

9 ²Instituto de Estudos Avançados, Universidade de São Paulo, São Paulo, Brazil

10 ³School of Geography, University of Leeds, Leeds, United Kingdom

11 ⁴Instituto de Geociências, Universidade de São Paulo, São Paulo, Brazil

12 ⁵Department of Geography, University of Leicester, Leicester, United Kingdom

13

14 *corresponding author: locosselli@yahoo.com.br

15

16 **Highlights:**

17 1) Water scarcity is one of the main challenges of the 21st century;

18 2) Water management must rely on records of climate and levels of water

19 reservoirs;

20 3) Intra-annual tree-ring oxygen isotope record seasonal variation in

21 precipitation amount;

22 4) The 2014 drought is recorded in the tree-ring oxygen isotopes across São

23 Paulo;

24 5) Tree-ring $\delta^{18}\text{O}$ values are a reliable record of water reservoir levels in the city;

25 **Abstract**

26 The impacts of climate change on precipitation and the growing demand for water
27 have increased the water risks worldwide. Water scarcity is one of the main challenges of
28 the 21st century, and the assessment of water risks is only possible from spatially
29 distributed records of historical climate and levels of water reservoirs. One potential
30 method to assess water supply is the reconstruction of oxygen isotopes in rainfall. We here
31 investigated the use of tree-ring stable isotopes in urban trees to assess spatial/temporal
32 variation in precipitation and level of water reservoirs. We analyzed the intra-annual
33 variation of $\delta^{13}\text{C}$ and $\delta^{18}\text{O}$ in the tree rings of *Tipuana tipu* trees from northern and southern
34 Metropolitan Area of São Paulo (MASP), Brazil. While variation in $\delta^{13}\text{C}$ indicates low leaf-
35 level enrichments from evapotranspiration, $\delta^{18}\text{O}$ variation clearly reflects precipitation
36 extremes. Tree-ring $\delta^{18}\text{O}$ was highest during the 2014 drought, associated with the lowest
37 historical reservoir levels in the city. The $\delta^{18}\text{O}$ values from the middle of the tree rings have
38 a strong association with the mid-summer precipitation ($r = -0.71$), similar to the association
39 between the volume of precipitation and its $\delta^{18}\text{O}$ signature ($r = -0.76$). These consistent
40 results allowed us to test the association between tree-ring $\delta^{18}\text{O}$ and water-level of the
41 main reservoirs that supply the MASP. We observed a strong association between intra-
42 annual tree-ring $\delta^{18}\text{O}$ and the water-level of reservoirs in the northern and southern MASP
43 ($r = -0.94$, $r = -0.90$, respectively). These results point to the potential use of high-resolution
44 tree-ring stable isotopes to put precipitation extremes, and water supply, in a historical
45 perspective assisting public policies related to water risks and climate change. The ability
46 to record precipitation extremes, and previously reported capacity to record air pollution,
47 place *Tipuana tipu* in a prominent position as a reliable environmental monitor for urban
48 locations.

49 Keyword: *Tipuana tipu*, dendrochronology, stable isotopes, water risk, drought,
50 tropics.

51

52 **Introduction**

53 Earth's rising temperature is already producing profound changes in precipitation
54 regimes (IPCC 2013). These effects of climate change combined with the warmer
55 conditions found in the cities intensify the convective activity and the concentration of
56 precipitation, increasing the vulnerability of cities to rainfall anomalies (Muis et al 2015).]
57 Drought is one of the most common natural hazards in the cities worldwide (Gu et al. 2015,
58 Larsen et al 2016). Sustained low precipitation anomalies combined with poor
59 management of natural resources and high-water consumption in dense cities increase the
60 vulnerability of their supply systems (Larsen et al 2016). Water scarcity risk, or the
61 imbalance between availability and basic needs, is recognized as one of the main
62 challenges of the 21st century worldwide (Orr et al 2009), directly affecting water-dependent
63 economic activities and population's livelihood (Gu et al. 2015).

64 São Paulo, the 5th largest megacity in the world (UN 2016), is an example of such a
65 vulnerable place. Like many other mega-cities in developing countries, São Paulo is
66 already facing the combined challenges of unplanned growth and climate change. It is
67 under the influence of increased frequency of extreme rainfall and drought events
68 (Sugahara et al 2009, Marengo et al. 2020), severely affecting citizens lives. This city is
69 already struggling with consistent water supply shortage during long droughts. The year of
70 2014 was marked by one of the worst droughts events that resulted in a water supply crisis.
71 This crisis was caused by a sequence of drier years followed by an unusual mid-
72 troposphere blocking in 2014. This unusual climatic event resulted in the driest and
73 warmest summer since 1951, according to the available records (Nobre et al 2016).

74 Precipitation was not only limited during this year, but it was unevenly distributed across
75 the metropolitan area of São Paulo affecting mainly the northern part of the city, with
76 relatively minor effects in the south.

77 Spatiotemporal variability of extreme climate events, such as the one of 2014 in São
78 Paulo, are usually assessed using climate data from instrumental records (Taffarello et al.
79 2016). However, where such records are not available, alternative environmental archives
80 like tree rings may provide valuable insights. Stable oxygen and carbon isotopes in tree-
81 ring cellulose are reliable proxies to understand climate variability. So far, tree-ring $\delta^{18}\text{O}$ in
82 the tropics often shows negative relationship with the precipitation volume and thus
83 provides a record of local and regional precipitation variability (Baker et al. 2015, 16,
84 Brienen et al 2012, 2013). This can be explained by an enhanced removal of heavy
85 isotopes (H_2O^{18}) along the trajectory of water vapor from the original water source to the
86 site of condensation, modulated by the intensity of the precipitation events locally
87 (Dansgaard 1964, Risi et al. 2008). The rainfall signal in the tree rings also depends on
88 whether the relationship between source $\delta^{18}\text{O}$ and precipitation volume dominates over the
89 influence of leaf physiology on tree-ring $\delta^{18}\text{O}$, which is primarily a result of variations in
90 Vapor Pressure Deficit (VPD, Barbour et al 2004, Kahmen et al 2011, Cintra et al 2019).
91 This influence of VPD on stomatal opening can be indirectly assessed using the carbon
92 isotopes. The tree-ring $\delta^{13}\text{C}$ depends on the fractionation during CO_2 diffusion through the
93 stomata, and assimilation by the RUBISCO activity (Farquhar et al 1982). Tree-ring carbon
94 isotopic patterns may also be related to the use of carbon reserves during growth (Eglin et
95 al. 2010). Both oxygen and carbon stable isotopes are usually analyzed at inter-annual
96 basis (McCarroll and Loader 2004), but they may be as well analyzed at intra-annual basis
97 to allow a comprehensive understanding of the intra-seasonal variation of climate
98 conditions (Helle and Schleser 2004, Monson et al 2018) likely providing detailed

99 information for risk assessments. Surprisingly, there are no studies about climatic
100 variability in the cities based on tree-ring stable isotopes, despite the fact that many
101 developing countries, that concentrate 82% of the world's megacities (UN 2018), only have
102 limited data to effectively manage their water resources (Kirby and Ahmad 2015).

103 The aim of this study is to evaluate the potential of using high-resolution stable
104 isotopes in tree rings of urban trees to assess spatial / temporal variability in precipitation
105 extremes, a key information to support management of water shortage risk in the cities.
106 We used the Metropolitan Area of São Paulo as a case study because it has a large
107 distribution of trees (Silva et al. 2019), specifically of *Tipuana tipu* (Benth.) Kuntze, with
108 proven annual rings (Locosselli et al. 2019), a large network of climate stations, as well as
109 records of the levels of water reservoirs. Based on this context, we analyzed both oxygen
110 and carbon stable isotopes in ten segments of each tree ring produced between 2010 and
111 2015 for a total of six trees from northern and southern São Paulo. We tested the following
112 hypotheses: 1) There is a negative relationship between $\delta^{18}\text{O}$ signature of precipitation and
113 its volume in the city; 2) Tree-ring $\delta^{18}\text{O}$ records are not affected by elevated
114 evapotranspiration due to VPD; 3) The $\delta^{13}\text{C}$ series also indicate a low influence of leaf-
115 water enrichment in the isotope signal of source water; and 4) Tree-ring $\delta^{18}\text{O}$ is a reliable
116 record of monthly precipitation volume across the city. If indeed hypotheses one to four are
117 confirmed, then 5) *T. tipu* tree-ring $\delta^{18}\text{O}$ records can be used as a proxy for past
118 precipitation volume and likely for past level of water reservoirs that supply the city.

119

120 **Material and Methods**

121

122 **Study Sites**

123

124 Sites are located 20 km apart in the Metropolitan Area of São Paulo, Brazil (MASP,
125 Figure 1). One site is located in the north at the Santa Amélia Public Park (23°30'00"S,
126 46°22'28"W, 777m a.s.l.) and the other one is located in the south at Capuava (23°40'00"S,
127 46°27'47"W, 775m a.s.l.). The climate in São Paulo is seasonal, with a clear rainy season
128 extending roughly from September to March. Most of the air masses that bring precipitation
129 to the city, and its water reservoirs, come from the South Atlantic during the rainy season,
130 with minor influence from other regions (Figure S1). The northern site is comparatively
131 warmer and drier than the southern site (Figure S2), and it had 18% less monthly
132 precipitation compared to the south during the drought of 2014 (Figure 1). This anomaly
133 extended over a large region to the north of São Paulo city mainly affecting the precipitation
134 over the Cantareira reservoir system (Pattnayak et al 2018, Figure 1), with relatively minor
135 effects over the Rio Grande reservoir system in the south. The Cantareira system, the
136 largest one in the MASP with a catchment area of ca. 2,303 km², has a storage capacity
137 of almost 1 trillion liters of water and supplies 6.5 million people in the region, while the Rio
138 Grande system, with a catchment area of ca. 583 km², stores more than 11 billion liters of
139 water and supplies more than 1.2 million people (SABESP 2020).

140

141 **$\delta^{18}\text{O}$ analyses of rainfall water**

142

143 To establish whether precipitation $\delta^{18}\text{O}$ records correlate with cumulated
144 precipitation amount in the Metropolitan Area of São Paulo, we analyzed the monthly
145 variation in precipitation $\delta^{18}\text{O}$ for a period of 16 months (from January 2004 to April 2005).
146 Precipitation samples were obtained at the Institute of Geosciences, University of São
147 Paulo, located in between both sampling sites. Water samples were obtained monthly
148 using a tube-dip-in-water collector with pressure equilibration system, according to

149 IAEA/GNIP (2014). Samples were analyzed with mass spectrometer IRMS (DeltaPlus
150 Advantage from Thermo Fischer) attached to a Gas-Bench-II System and using the CO₂-
151 water equilibrium technique. The uncertainties for $\delta^{18}\text{O}$ is 0.5 ‰. We tested the relationship
152 between rainfall $\delta^{18}\text{O}$ and precipitation volume (obtained from the climate station at the
153 Institute of Astronomy and Geophysics, also in the University of São Paulo) using
154 Pearson's correlation.

155

156 **Study species and tree-ring sampling**

157

158 For the present study, we analyzed trees from the species *Tipuana tipu* (Benth.)
159 Kuntze (Fabaceae) which is one of the three most common species in the metropolitan
160 region of São Paulo (Moreira et al 2018). Because it is so well adapted to the urban
161 environment, it has also been planted in cities from South and Northern America, Europe,
162 Africa, Asia and Oceania (Moreira et al 2018). It is considered deciduous for shedding all
163 leaves during the dry season, and the trees have a shallow root system usually visible at
164 the soil surface (Locosselli et al. 2018). It has distinct semi-porous rings delimited by a
165 marginal parenchyma band (Locosselli et al 2019) that are formed during the rainy season.
166 It is important to note that trees used in this study obtained their water from rainfall without
167 any additional water input from irrigation systems.

168 Two to four increment cores were obtained from each tree, using 5mm increment
169 borers. A total of seven trees were sampled at the northern site specifically for the present
170 study, while 41 trees were previously sampled in the southern site (Locosselli et al. 2019).
171 Data of tree diameter at breast height (DBH), tree height, overall conditions of the tree and
172 geographical coordinates were recorded in the field. Injuries to tree stems due to coring
173 were treated with a saturated solution of copper sulphate and calcium carbonate to avoid

174 later infections. We fixed the samples in wood supports and left them to dry for a couple of
175 weeks.

176

177 **Tree-ring sample preparation**

178

179 We sanded all samples using sandpaper with grits ranging from 60 to 2000, and
180 identified the tree-ring boundaries. All samples were then scanned using a high-resolution
181 scanner (Epson v33). Samples from the south had been cross-dated in a previous study
182 using standard dendrochronological methods (Locosselli et al. 2019), while the tree-rings
183 series from the northern population were only cross-dated within each individual because
184 of the small sample collection. Among the available samples from both sites, we chose
185 three trees with wide tree rings in each site for the intra-annual isotope analysis. The
186 chosen trees from the north and south have in average, 54.00 and 76.37 cm of DBH, 10.37
187 and 13.67 m of height and 31 and 33 years old, respectively. We produced transversal
188 sections with 2mm width from the increment cores using a circular saw (Proxxon KS 230,
189 Saw Blade 28 020). We isolated segments from the thin sections containing the years
190 between 2010 to 2015.

191 To extract the cellulose, segments were placed inside supports made with
192 perforated Teflon sheets, and treated twice with 5% NaOH solution for 2 hours (4 hours
193 total) in the water bath at 60°C to remove resins, fatty acids and tannins. We then washed
194 the samples with de-ionized boiling water, and treated them with 7,5% NaClO₂ solution
195 with a pH of 4-5 in the water bath at 60°C for 37 hours. Finally, we washed the samples
196 once again with de-ionized boiling water and dried the holo-cellulose samples in a freeze-
197 dryer (Kagawa et al 2015, Schollaen et al. 2017).

198

199 **Tree-ring isotope analyses**

200

201 From the holo-cellulose samples, 10 sections were analyzed for $\delta^{13}\text{C}$ and $\delta^{18}\text{O}$ from
202 each ring. Because cambium activity is not constant throughout the growing season (e.g.
203 Marcati et al 2008) and because we expect that variation in the wood density reflects more
204 closely the cambium activity during the growth season, we did not divide rings into sections
205 of equal width but in sections of equal weight. Thus, sections with higher wood density,
206 which we expect to be formed during period of slower radial growth, were sampled at
207 slightly higher spatial resolution (i.e, smaller width of ring sections, see Fig, 2). For the
208 isotope analysis, between 450 and 550 μg of cellulose were packed into silver cups for
209 $\delta^{18}\text{O}$, and between 900 and 1100 μg of cellulose were packed in tin cups for $\delta^{13}\text{C}$, resulting
210 in a total of 720 samples. Samples were pyrolyzed at 1400°C over glassy carbon on a
211 Sercon HT furnace interfaced to a 20-20 isotope ratio mass spectrometer.

212

213 **Intra-annual isotope series synchronization**

214

215 The stable isotope series showed highly similar intra-annual variation in the same
216 rings between trees (Figure S3). However, the intra-annual positions of highest and lowest
217 isotope values were not exactly the same for different trees, most likely due to slight
218 differences between trees in radial growth rates over their active growing season. Simple
219 averaging procedures would mix isotope values from slightly different periods. Thus, to
220 create a mean average intra-annual time series, in which each intra-annual sample point
221 corresponded to the exact timing of wood formation in all trees, we synchronized apparent
222 temporal mismatches between trees. To this end, we moved every series a number of
223 positions to the left and to the right so that the high and low values of $\delta^{18}\text{O}$ would match in

224 time (Figure S4). Most of the years required moving the relative position of the oxygen
225 isotope series only by one position to the left or to the right, while others only required
226 moving two positions. We did not merged segments nor split any series for synchronization.

227 We calculated the GLK value (Gleichläufigkeit, Bura & Wilmking 2015) to check the
228 synchronicity of the series ('dplR', Bunn, 2008), and calculated the average intra-annual
229 $\delta^{18}\text{O}$ series for each year at each site. We only used the average series calculated from
230 the values of at least two trees, and all average series have ten values of intra-annual
231 isotopes. We adjusted the $\delta^{13}\text{C}$ values according to the positions of the synchronized $\delta^{18}\text{O}$
232 series for calculating the mean series. For the $\delta^{13}\text{C}$, we standardized the dataset using z-
233 scores before averaging ($\text{mean } \delta^{13}\text{C} - \text{position } \delta^{13}\text{C} / \text{standard deviation}$), because of the
234 strong variation in the mean $\delta^{13}\text{C}$ among trees, presumably caused by variation between
235 trees in height, light exposure and water availability (Fichtler et al. 2010, Brienen et al.
236 2017, Cintra et al 2019).

237

238 **Association between isotopic series, climate and level of water reservoirs**

239

240 To assess the effects of climate on the isotope series, we used correlation analyses
241 between isotope values and monthly precipitation and VPD data and presented these as
242 heatmaps. This was done by combining the northern and southern populations datasets
243 in a single analysis (so, 12 values of isotopes and 12 values of climate per month,
244 equivalent to the 6 rings in the two sites), thus taking into account the temporal trends plus
245 possible variation in rainfall and VPD between sampling sites. We calculated Pearson's
246 correlation values between all combinations of mean isotope ratios at each position within
247 the tree ring (from 1 to 10) and the monthly precipitation and VPD in the north and south.
248 Climate datasets were obtained from the National Institute of Meteorology (INMET, Mirante

249 de Santana climate Station) to represent the climate in Northern São Paulo, and from the
250 Institute of Astronomy and Geophysics (IAG, University of São Paulo, Cientec Park climate
251 station) to represent Southern São Paulo. Based on the relationship between the stable
252 isotopes and the climate data, we aligned the intra-annual variation of both oxygen and
253 carbon isotopes and the climate series according to the results presented in the heatmaps.
254 We then plotted the average tree-ring $\delta^{18}\text{O}$ and $\delta^{13}\text{C}$ over the precipitation and VPD series,
255 aligning their position 5 (out of the 10 positions) with January, the middle of the rainy
256 season. Please refer to the results for further details.

257 We also tested if the intra-annual oxygen isotope values are reliable proxies for
258 water level in the reservoirs closest to the northern and southern sampling sites. We
259 evaluated the linear relationship between $\delta^{18}\text{O}$ from position 5 and monthly values of water
260 level in the reservoirs (Cantareira System in the north, and Rio Grande System in the south,
261 data from SABESP) for the period between July of the current calendar year to December
262 of the next calendar year, a total of 18 months, as the effects of precipitation on the water-
263 levels may be lagged by a few months (Figure 1). Linear relationships were tested
264 independently for the Northern and Southern populations as they depend also on the
265 physical characteristics of the catchment area and the reservoir, and differences in
266 consumption demand. Results were plotted for the month with the highest correlation
267 values in each site.

268

269 **Results**

270

271 We find that there is a significant negative relationship between monthly
272 precipitation and rainfall $\delta^{18}\text{O}$ ($r = -0.76$, $p = 0.0006$; Figure 3) during the 16 months of
273 measurements in central São Paulo. The highest (0.20 ‰) and lowest (-8.80 ‰) rainfall

274 $\delta^{18}\text{O}$ values were observed in the months of January and August corresponding to the
275 middle of the rainy and dry seasons, respectively. It is also possible to observe in Figure 3
276 that part of the $\delta^{18}\text{O}$ variation is not explained by the variation in precipitation volume in the
277 Metropolitan Area of São Paulo, especially in the transition periods between the dry and
278 wet seasons.

279 The variation in the oxygen isotope values within individual rings can be as high as
280 6.7 ‰ in the north and 5.5 ‰ in the South. Across all years and data-points, the highest
281 $\delta^{18}\text{O}$ value is found in all sampled trees in the middle of the growing season represented
282 by the tree ring formed between 2013 and 2014, corresponding to the drought of 2014 in
283 the city. Even the lowest values in this year barely drop below 28 ‰. The intra-annual
284 patterns of $\delta^{13}\text{C}$ are also consistent among the sampled trees of each site, but they differ
285 between sites (Figure S3). At the northern site, the lowest values of $\delta^{13}\text{C}$ are found at the
286 beginning and end of the tree rings, with the highest values at the middle of it. In contrast,
287 in the southern site, the values of $\delta^{13}\text{C}$ gradually decrease from the beginning to the end
288 of the tree ring. We observed only moderate to low correlation values between the intra-
289 annual variations of $\delta^{13}\text{C}$ and $\delta^{18}\text{O}$ among the individuals from the south and north of the
290 Metropolitan Area of São Paulo (Figure S5, $r = -0.42$ and $r = -0.28$, respectively).

291 The series of $\delta^{18}\text{O}$ showed a consistent improvement in the GLK values after the
292 synchronization (Table 1, Figures S6 to S9). Using the average synchronized series, we
293 found a strong negative correlation between the mean $\delta^{18}\text{O}$ at position 5 within the tree
294 rings and precipitation variability of January across sampling sites ($r = -0.71$, $p = 0.01$,
295 Figure 4), but no significant correlations between $\delta^{18}\text{O}$ and VPD. This observed pattern of
296 association between $\delta^{18}\text{O}$ from the middle of the tree ring and precipitation from mid-
297 summer is also consistent when evaluating the populations separately (Figures S10 and
298 S12), and therefore not dependent on site conditions. On the other hand, the synchronized

299 series of $\delta^{13}\text{C}$ showed a negative correlation between the isotope values in position 4, 5
300 and 6 and the precipitation of December, January and February ($r = - 0.69$, $p = 0.01$; $r = -$
301 0.64 , $p = 0.02$; $r = - 0.69$, $p = 0.01$ respectively, Figure 4). In contrast to $\delta^{18}\text{O}$, we find a
302 significant negative correlation between the $\delta^{13}\text{C}$ values from positions 1, 2, and 3 and the
303 VPD for all tested months (up to $r = - 0.79$, $p = 0.002$), and positive correlations for the
304 positions 5, 6 and 7 (up to $r = 0.87$, $p = 0.0002$). In contrast to the results found with the
305 $\delta^{18}\text{O}$, the ones found with $\delta^{13}\text{C}$ seem to be more dependent on the variability of site
306 conditions (Figures S10 and S11). A level of independency among the different intra-
307 annual samples could be observed as the isotope values presented significant correlations
308 with only the neighboring positions within each tree ring (Figure S13), as well as low
309 correlation values between mean intra-annual $\delta^{13}\text{C}$ and $\delta^{18}\text{O}$.

310 Because of the significant association between precipitation volume and $\delta^{18}\text{O}$
311 values from the tree ring, especially at position 5, we tested the correlation between tree-
312 ring $\delta^{18}\text{O}$ and the levels of water reservoirs. Although no significant correlation was
313 observed between the average tree-ring $\delta^{18}\text{O}$ values and the level of the water-reservoirs
314 ($r = - 0.71$, $p = 0.11$; and $- 0.68$, $p = 0.14$ for the north and south sites, respectively, Figure
315 S15), there is a strong linear relationship between the level of the water reservoirs and
316 $\delta^{18}\text{O}$ values from tree-ring position 5 ($r = - 0.94$, $p = 0.005$; and $- 0.90$, $p = 0.01$ for the north
317 and south sites, respectively, Figure 6). This latter association also holds up when
318 averaging the $\delta^{18}\text{O}$ values of positions 5 and 6, but with a less strong linear relationship (r
319 $= - 0.89$, $p = 0.02$; and $- 0.85$, $p = 0.03$ for the north and south sites, respectively, Figures
320 S16).

321

322 Discussion

323

324 The consistent patterns of intra-annual stable isotopes in the tree rings of the
325 sampled trees further support previous findings from Locosselli et al. (2019) that these
326 rings are formed annually. These common patterns likely became more evident in the intra-
327 annual series due to our strategy of dividing every tree ring into the same number of
328 segments, with similar weight instead of similar width. The initial mismatches observed in
329 the intra-annual isotope series among trees from the same site (see Figure S3) probably
330 suggest that individual trees may start or stop growing at slightly different times during the
331 growing season, and/or differ in seasonal variation in radial growth. Indeed, in the tropics,
332 relatively low synchrony in phenological and physiological processes during the vegetative
333 period has been observed (Bosio et al 2016, Lara & Macarti 2016, Marcati et al. 2016,
334 Vogado et al. 2016). After minor shifts in the intra-annual series, a position to the left or to
335 the right, we do find very strong common intra-annual isotopic signal for $\delta^{18}\text{O}$ among trees,
336 with uniquely different patterns among years (see Figure S4 to S6). This suggests that,
337 indeed, initial mismatches between exact peaks and lows of $\delta^{18}\text{O}$ are caused by slight
338 differences in growth rhythms among trees.

339 It is during the middle of the growing season, when we observed the strongest
340 association between tree-ring $\delta^{18}\text{O}$ and precipitation volume in both sampling sites. This
341 association is in accordance with the negative effect of monthly precipitation amount on
342 $\delta^{18}\text{O}$ signature of São Paulo's rainfall. The strong source signal in the tree-rings $\delta^{18}\text{O}$ is
343 further supported by the similarity of the calculated Pearson's correlation values between
344 precipitation volume and its $\delta^{18}\text{O}$ signature ($r = -0.76$), and between precipitation volume
345 and tree-ring $\delta^{18}\text{O}$ values ($r = -0.71$). The observed intra-annual tree-ring $\delta^{18}\text{O}$ values
346 reflect important precipitation extremes as those recorded during the summer of 2011 in
347 the north, and especially the drought of 2014 in the north and in the south (Figure 5). A
348 similarly strong source-water signal in the tree rings has been observed in several natural

349 populations of trees, from tropical and extratropical regions (e.g. Zhu et al. 2012, Brienen
350 et al 2012, 2013, Baker et al 2015, 2016, Xu et al. 2016, Cintra et al. 2019), especially in
351 conditions with low evaporative demand that result in low leaf-water enrichment. This
352 strong association with the source water signal, however, has not been observed in cities
353 before. Surprisingly, we did not observe a significant effect of leaf-water enrichment on the
354 source-water signal even under the high evaporative conditions found in São Paulo (Silva
355 et al. 2019). At least not during the vegetative period that takes place along the wettest
356 months of the year. This observation is also supported by the low association between
357 tree-ring $\delta^{18}\text{O}$ and VPD. The strong precipitation signal in the tree-rings $\delta^{18}\text{O}$ may also be
358 a consequence of the shallow root system of *T. tipu* (Locosselli et al. 2018) that may reduce
359 the mixing with deep water sources.

360 The lack of significant influence of leaf-water enrichment, mainly due to
361 evapotranspiration, on tree-ring $\delta^{18}\text{O}$ records is also supported by the low association
362 between intra-annual $\delta^{13}\text{C}$ and $\delta^{18}\text{O}$ variation (Cintra et al 2019). The results also indicate
363 that intra-annual $\delta^{13}\text{C}$ variability mainly reflects different strategies of carbon allocation in
364 the north and in the south. A decreasing trend of $\delta^{13}\text{C}$ from earlywood to latewood, as
365 observed in the south, has been widely described in the literature. This pattern is often
366 related to the remobilization of non-structural carbohydrates, mainly starch, to support
367 growth in the early vegetative period, leading to relative high values in early ring sections
368 (Helle and Schleser 2004, Cernusak et al 2009, Eglin et al. 2010). Trees then may leave
369 their stomata open from the middle to the end of the wet season to support assimilation,
370 leading to decreases in $\delta^{13}\text{C}$ values (as assimilation is less restricted by stomatal
371 conductance). This pattern, however, was not observed in the north, where trees had high
372 values of $\delta^{13}\text{C}$ in the middle of the tree ring. These differences are likely related to the
373 spatial variability of VPD in São Paulo, with generally drier conditions in the north. This

374 control is evident from the negative correlation of all monthly VPD values with the tree-ring
375 $\delta^{13}\text{C}$ from position 1, 2 and 3, and positive correlations with the $\delta^{13}\text{C}$ from positions 5, 6
376 and 7. This implies that VDP is likely controlling the shape of the $\delta^{13}\text{C}$ curve along the
377 growth season, and likely the strategies of carbon allocation and mobilization. While low
378 VPD will result in a descending curve as observed in the south, high VPD will result in an
379 inverted “U” curve as observed in the north. The inverted “U” curve was also replicated in
380 most sampled trees during the drought of 2013-2014 that resulted in a high VPD across
381 the city (Figure S3). The negative relationship between $\delta^{13}\text{C}$ and precipitation only during
382 December, January and February may imply that trees will only increase stomatal
383 conductance (McCarroll and Loader 2014) when water availability is at its highest.
384 Therefore, it confirms that even a high stomatal conductance during this period is unlikely
385 to add noise to the source-water signal recorded in the tree-rings $\delta^{18}\text{O}$.

386 Given the effect of the precipitation volume on its $\delta^{18}\text{O}$ signature combined with the
387 strong source-water signal in the tree rings, especially in position 5, we tested if tree-ring
388 $\delta^{18}\text{O}$ could be used as a record of the level of water-reservoirs in the city. The level of the
389 water reservoirs, that depends on the accumulated rainfall over the entire catchment
390 (Taffarello et al. 2016), is strongly associated with the tree-ring $\delta^{18}\text{O}$ from position 5 in trees
391 from north and south of the MASP ($r = - 0.94$ and $- 0.90$, respectively). A higher slope value
392 was observed in the linear fit for the northern population, probably due to the greater
393 distance from the Atlantic Ocean (main source of rainwater in the city, Figures 1 and S1),
394 the greater observed variability in the volume of rainfall, and the resulting greater range in
395 water level variability in the Cantareira system, when compared to that observed in the
396 south. The observed relationship between water level of the reservoirs and tree-ring $\delta^{18}\text{O}$
397 emerges much more clearly when using our approach of analyzing a fixed number of
398 segments per year, in this case 10 segments, than by analyzing the average $\delta^{18}\text{O}$ value of

399 the entire tree ring. This association demonstrates the potential of using the intra-annual
400 oxygen isotopes to reconstruct the levels of the water reservoirs in the city, especially
401 during drought events such as the one of 2014 (Nobre et al 2016). For a more practical
402 application, it is also possible to use a large sample of the tree rings, corresponding to the
403 combined positions 5 and 6, roughly the middle of the tree ring, for obtaining a reliable
404 record of the levels of the water reservoirs. This strong association also suggests that tree-
405 ring oxygen isotopes not only reflects local precipitation, but they integrate the volume of
406 precipitation and its isotopic signal over the extensive area of the reservoirs' catchment.

407 In summary, this is the first study to show the potential of using intra-annual stable
408 isotopes in trees as a reliable record of precipitation extremes. While the tree-ring $\delta^{13}\text{C}$
409 recorded mainly physiological processes related to carbon allocation and mobilization, the
410 $\delta^{18}\text{O}$ records found in the tree rings of *Tipuana tipu*, a tree species common to cities from
411 South and North America, Europe, Africa, Asia and Oceania (Moreira et al. 2018), stand
412 out as a reliable instrument to assist the assessment of water resources risks for locations
413 with poor historical records. The results show a clear association with monthly precipitation
414 in both temporal and spatial scales, being able to record heavy precipitation events as in
415 the year of 2011 and the drought of 2014, while being a reliable proxy for assessing the
416 level of the water reservoirs in the city. This approach has the potential to be also used to
417 find how singular, or frequent, events like the 2014 drought are in the city, given that
418 specimens of *T. tipu* planted in the early 20th century are still found in São Paulo (Brazolin
419 2009). *Tipuana tipu* is emerging as a trustworthy environmental monitor for urban areas
420 due to its capacity to record both spatial and temporal variation in air pollution, as
421 previously reported (Geraldo et al. 2014, Locosselli et al. 2018, Moreira et al. 2018,
422 Locosselli et al. 2020), with the ability to record precipitation extremes and the level of
423 water reservoirs, as shown in the present study.

424

425 **Acknowledgement**

426

427 Authors thank the “Secretaria do Verde e do Meio Ambiente / PMSP” for the permit
428 for sampling the trees in the public parks, and also Prosecutor José Luiz Saikali for
429 providing the authorizations required to sample the trees in Southern São Paulo. We also
430 thank Plácido Buarque, Fabio Machado Coelho and Rafael Santos Saraiva for helping with
431 field work, and Dr Mario Tomasello and Msc Daigard Ricardo Ortega Rodriguez for helping
432 with the X-ray densitometry analysis, and Dr Bruno Cintra for the valuable insights on the
433 analyses. This study was supported by the São Paulo Research Foundation (FAPESP
434 2004/05360-6, 2010/20876-0, 2013/21728-2, 2015/25511-3, 2017/10544-9, 2017/50085-
435 3, 2018/22422-8, 2019/08783-0), CNPq (304126/2015-2) and Higher Education
436 Improvement Coordination (CAPES).

437

438 **References**

439

440 Baker JCA, Hunt SFP, Clerici SJ et al. (2015) Oxygen isotopes in tree rings show
441 good coherence between species and sites in Bolivia. *Global Planet Change* 133:298–
442 308.

443 Baker JCA, Gloor M, Spracklen DV, Arnold SR, Tindall JC, Clerici SJ, Leng MJ,
444 Brienen RJW (2016) What drives interannual variation in tree ring oxygen isotopes in the
445 Amazon? *Geophys Res Lett* 43:11831–11840.

446 Barbour MM, Roden JS, Farquhar GD, Ehleringer JR (2004) Expressing leaf water
447 and cellulose oxygen isotope ratios as enrichment above source water reveals evidence
448 of a Péclet effect. *Oecologia* 138: 426–435.

449 Bosio F, Rossi S, Marcati CR (2016) Periodicity and environmental drivers of apical
450 and lateral growth in a Cerrado woody species. *Trees structure and Function* 30:1495-505

451 Brazolin S (2009) Biodeterioration, wood anatomy and falling risk analysis of
452 tipuana, *Tipuana tipu* (Benth.). *O. Kuntze trees, in the sidewalks of São Paulo city, SP.*
453 PhD Thesis, ESALQ – University of São Paulo, Piracicaba, São Paulo, Brazil, 265pg.

454 Brienens RJW, Gloor E, Clerici S, Newton R, Arppe L, Boom A, Botrell S, Callaghan
455 M, Heaton T, Helama S, Helle G, Leng MJ, Mielikäinen K, Oninonen M, Timonen M (2017)
456 Tree height strongly affects estimates of water-use efficiency responses to climate and
457 CO₂ using isotopes. *Nature Communications* 8: 288.

458 Brienens RJW, Hietz P, Wanek W, Gloor M (2013) Oxygen isotopes in tree rings
459 record variation in precipitation $\delta^{18}\text{O}$ and amount effects in the south Mexico. *Journal of*
460 *Geophysical Research: Biogeosciences* 118: 1-12.

461 Brienens RJW, Helle G, Pons TL, Guyot J, Gloor M (2012) Oxygen isotopes in the
462 tree rings a good proxy for Amazon precipitation and El Niño-Southern Oscillation
463 variability. *Proceedings of the National Academy of Sciences* 109: 16957-16962.

464 Bunn AG (2008) A dendrochronology program library in R (dplR).
465 *Dendrochronologia* 26(2), 115-124.

466 Bura A, Wilmking M (2015) Correcting the calculation of the Gleichläufigkeit.
467 *Dendrochronologia* 34: 29-30.

468 Cernusak LA, Tcherkez G, Keitel C et al. (2009) Why are nonphotosynthetic tissues
469 generally ¹³C enriched compared with leaves in C₃ plants? Review and synthesis of
470 current hypotheses. *Funct Plant Biol* 36:199–213.

471 Cintra BBL, Gloor M, Boom A, Schöngart J, Locosselli GM, Brienens R (2019)
472 Contrasting controls on tree ring isotope variation for Amazon floodplain and terra firme
473 trees. *Tree Physiology* 39: 845-860.

474 Dansgaard W (1964) Stable isotopes in precipitation. *Tellus XVI* 4: 436-468.

475 Eglin T, Francois C, Michelot A, Delpierre N, Damesin C (2010) Linking intra-
476 seasonal variations in climate and tree-ring $\delta^{13}\text{C}$: A functional modelling approach.
477 *Ecological Modelling* 221: 1779-1787.

478 Farquhar GD, O'Leary MH, Berry JA (1982) On the relationship between carbon
479 isotope discrimination and intercellular carbon dioxide concentration in leaves. *Australian*
480 *Journal of Plant Physiology* 9: 121–137.

481 Fichtler E, Helle G, Worbes M (2010) Stable-carbon isotope time series from tropical
482 tree rings indicate a precipitation signal. *Tree-Ring Research*, 66: 35-49.

483 Geraldo, S.M., Canteras, F.B., Moreira, S., 2014. Biomonitoring of environmental
484 pollution using tree rings of *Tipuana tipu*: quantification by synchrotron radiation total
485 reflection X-ray fluorescence. *Radiat. Phys. Chem.* 95, 346e348.

486 Gu D, Gerland P, Pelletier F, Cohen B (2015) Risks of exposure and vulnerability
487 to natural disasters at the city level: a global overview. United Nations, Technical Paper
488 N°2015/2.

489 Helle G and Scheleser GH (2004) Beyond CO_2 fixation by Rubisco – an
490 interpretation of $^{13}\text{C}/^{12}\text{C}$ variations in the tree rings from intra-seasonal studies on broad-
491 leaf trees. *Plant Cell and Environment* 27: 367-380.

492 Intergovernmental Panel on Climate Change. *Climate Change (2013) The Physical*
493 *Science Basis. Contribution of Working Group I to the Fifth Assessment Report of the*
494 *Intergovernmental Panel on Climate Change (eds Stocker, T. F. et al.) (Cambridge Univ.*
495 *Press, 2013).*

496 IAEA/GNIP – International Atomic Energy Agency & Global Network on Isotope
497 Precipitation (2014). *Precipitation sampling guide (V2.02 September) A new device for*

498 monthly rainfall sampling for GNIP. Water & Environment News Letter, 16, November,
499 Vienna.

500 Kagawa A, Sano M, Nakatsuka T, Ikeda T, Kubo S (2015) An optimized method for
501 stable isotope analysis of tree rings by extracting cellulose from cross-sectional laths.
502 Chemical Geology 393-394: 16-25.

503 Kahmen A, Sachse D, Arndt SK, Tu KP, Farrington H, Vitousek PM, Dawson TE
504 (2011) Cellulose $\delta^{18}\text{O}$ is an index of leaf-to-air vapor pressure difference (VPD) in tropical
505 plants. Proc Natl Acad Sci USA 108:1981–1986.

506 Kirby M, Ahmad MD (2015) Water resources management in developing countries:
507 the role of hydrology–economic modelling. CSIRO Land and Water Report, Australia. 38
508 pg.

509 Lara NOT, Marcati CR (2016) Cambial activity lasts 9 months in a tropical evergreen
510 species. Trees Structure and Function 30: 1331-1339.

511 Larsen TA, Hoffmann S, Lüthi C, Truffer B, Maurer M (2016) Emerging solutions to
512 the water challenges of an urbanizing world. Science 352: 928-933.

513 Locosselli GM, Chacón-Madrid K, Arruda MAZ, Camargo EP, Moreira TC, André
514 CDS, André PA, Singer JM, Saldiva PHN, Buckeridge MS (2018) Tree rings reveal the
515 reduction of Cd, Cu, Ni and Pb pollution in the central region of São Paulo, Brazil.
516 Environmental Pollution v. 242, p. 320-328, 2018.

517 Locosselli GM, Camargo EP, Moreira TCL, Todesco E, Andrade MF, André CDS,
518 André PA, Singer JM, Ferreira LS, Saldiva PHN, Buckeridge MS (2019) The role of air
519 pollution and climate on the growth of urban trees. Science of Total Environment 666: 652-
520 661.

521 Locosselli GM, Moreira TCL, Chacón-Madrid K, Arruda MAZ, Camargo EP,
522 Kamigauti L Y, Trindade RIF, Andrade MF, André CDS, André PA, Singer JM, Saiki M,

523 Zacarelli-Marino MA, Saldiva PHN, Buckeridge MS (2020) Spatial-temporal variability of
524 metal pollution across and industrial district, evidencing the environmental inequality in São
525 Paulo. Environmental Pollution DOI: 10.1016/j.envpol.2020.114583.

526 Marcati CR, Milanez CRD, Machado SR (2008) Seasonal development of secondary
527 xylem and phloem in *Schyzolobium parahyba* (Vell.) Blake (Leguminosae:
528 Caesalpinoideae). Trees, Structure and Function 22: 3-12.

529 Marcati CR, Machado SR, Podadera DS, Lara NOT, Bosio F, Wiedenhoeft AC
530 (2016) Cambial activity in dry and rainy season on branches from woody species growing
531 in Brazilian Cerrado. Flora 223:1-10

532 Marengo JA, Alves LM, Ambrizzi T, Young A, Barreto NJC, Ramos AM (2020)
533 Trends in extreme rainfall and hydrogeometeorological disasters in the Metropolitan Area
534 of São Paulo: a review. Annals of the New York Academy of Sciences DOI:
535 10.1111/nyas.14307

536 McCarroll D, Loader NJ (2004) Stable isotopes in tree rings. Quaternary Science
537 Reviews 23: 771-801.

538 Muis S, Güneralp B, Jongman B, Aerts JCJH, Ward PJ (2015) Flood risk and
539 adaptation strategies under climate change and urban expansion: A probabilistic analysis
540 using global data. Science of Total Environment 538: 445-457.

541 Monson RK, Szejner P, Belmecheri S, Morino KA, Wright WE (2018) Finding the
542 seasons in the tree ring stable isotope ratios. American Journal of Botany 105(5): 819-821.

543 Moreira TCL, Amato-Lourenço LF, Da Silva Gt, André CDS, André PA, Barrozo
544 LV, Singer JM, Saldiva PHN, Saiki M, Locosselli GM (2018) The use of tree barks to
545 monitor traffic related air pollution: A case of study in São Paulo – Brazil. Frontiers in
546 Environmental Science 6: 1-12.

547 Nobre CA, Marengo JA, Seluchi ME, Cuartas LA, Alves LM (2016) Some
548 characteristics and impacts of the drought and water crisis in the Southeastern Brazil
549 during 2014-2015. *Journal of Water Resources and Protection* 8: 252-262.

550 Orr S, Cartwright A, Tickner D (2009) Understanding water risks, a primer on the
551 consequences of water scarcity for government and business. WWF Water Security
552 Series, 39pg.

553 Pattnayak KC, Gloor E, Tindall JC, Brienen RJW, Barichivich J, Baker JCA,
554 Spracklen DV, Cintra BBL, Coelho CAS (2018) Adding new evidence to the attribution
555 puzzle of the recent water shortage over São Paulo (Brazil). *Tellus A: Dynamic*
556 *Meteorology and Oceanography*, 70: 1-14.

557 Risi C, Bony S, Vimeux F, Joutzel J (2001) Water-stable isotopes in the LMDZ4
558 general circulations model: Model evaluation for present-day and past climates and
559 applications to climatic interpretations of tropical isotopic records. *Journal of Geophysical*
560 *Research* 115: D12118.

561 Risi C, Bony S, Vimeux F (2008) Influence of convective processes on the isotopic
562 composition ($\delta^{18}\text{O}$ and δD) of precipitation and water vapor in the tropics: 2. Physical
563 interpretation of the amount effect. *Journal of Geophysical Research* 133: D19306.

564 SABESP 2020, Mananciais, <http://site.sabesp.com.br/>, accessed on June 24th 2020.

565 Silva EMF, Bender F, Monaco MLS, Smith AK, Silva P, Buckeridge MS, Elbl PM,
566 Locosselli GM (2019) O ambiente urbano como um novo ecossistema: a construção das
567 florestas urbanas pelo Estado e movimentos ativistas. *Revista de Estudos Avançados*
568 33(97): 81-101

569 Schollaen K, Baschek H, Heirinch I, Helle G (2015) Technical note: an improved
570 guideline for rapid and precise sample preparation of tree-ring stable isotope analysis.
571 *Biogeosciences* 12: 11587-11623.

572 Sugahara S, Rocha RP, Silveira R (2009) Non-stationary frequency analysis of
573 extreme daily rainfall in São Paulo, Brazil. *International Journal of Climatology* 29: 1339-
574 1349.

575 Tafarello D, Mohor GS, Calijuri MC, Mendiõdo EM (2016) Field investigations of
576 the 2013-2014 drought through quali-quantitative freshwater monitoring at the headwaters
577 of the Cantareira System, Brazil. *Water International* 41(5): 776-800

578 United Nations (2018) *The World's Cities in 2018. – Data Booklet (ST/ESA/ SER.A/417)*.

579 Vogado NO, Camargo MGG, Locosselli GM, Morellato P (2016) Edge effects on the
580 phenology of the Guamirim, *Myrcia guianensis* (Myrtaceae), a Cerrado tree, Brazil.
581 *Tropical Conservation Science* 9:291-312.

582 Vuille 2018 Current and future challenges in stable isotope applications of the
583 tropical hydrological cycle. *Hydrological Processes* 32: 1313-1317.

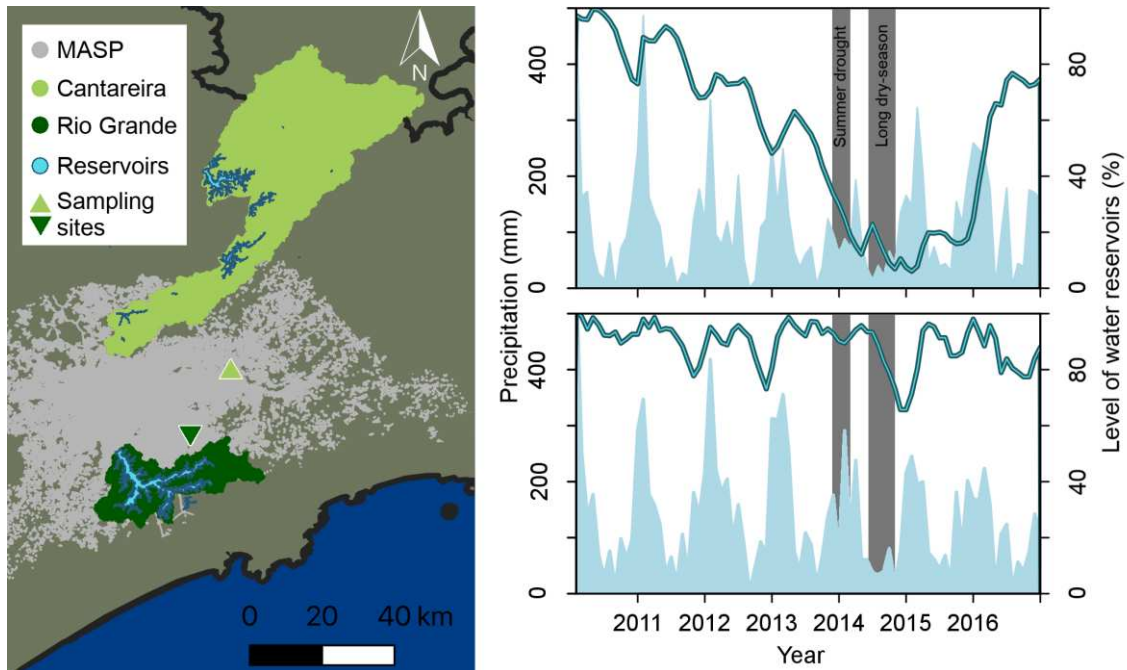
584 Xu C, Zheng H, Nakatsuka T, Sano M, Li Z, Ge J (2016) Inter- and intra-annual tree-
585 ring cellulose oxygen isotope variability in response to precipitation in Southeast China.
586 *Trees, Structure and Function* 30: 785-792.

587 Zhu M, Stott L, Buckley B, Yoshimura K, Ra K (2012) Indo-Pacific Warm Pool
588 convection and ENSO since 1867 derived from Cambodian pine tree cellulose oxygen
589 isotopes. *Journal of Geophysical Research* 117: D11307

590

591 Figures

592

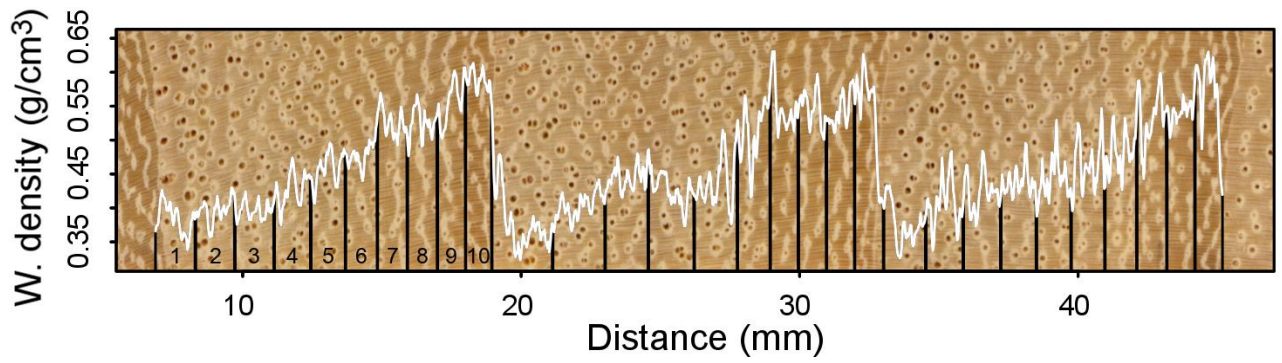


593

594 Figure 1: Sampling sites in northern (light green triangle) and southern (dark green
595 triangle) Metropolitan Area of São Paulo (MASP, in grey), Brazil. Monthly
596 precipitation (blue shaded area) from northern (upper panel) and southern (lower
597 panel) sampling sites are provided and the levels of water reservoirs (blue line)
598 closest to the sampling sites (Cantareira catchment in the north and Rio Grande
599 catchment in the South, data from Alto Tietê Drainage Basin Committee). One of
600 the strongest drought events in São Paulo occurred between 2013 and 2014
601 followed by a long dry-season in 2014 affecting the water supply in the entire
602 MASP. Climate data were obtained from SABESP (Companhia de Saneamento
603 Básico do Estado de São Paulo), INMET (National Institute of Meteorology of
604 Brazil) and IAG/USP (Institute of Astronomy, Geophysics, and Atmospheric
605 Sciences of the University of São Paulo, University of São Paulo).

606

607



608

609

610 Figure 2: Example of the wood density profile (white) of three tree rings of *Tipuana*

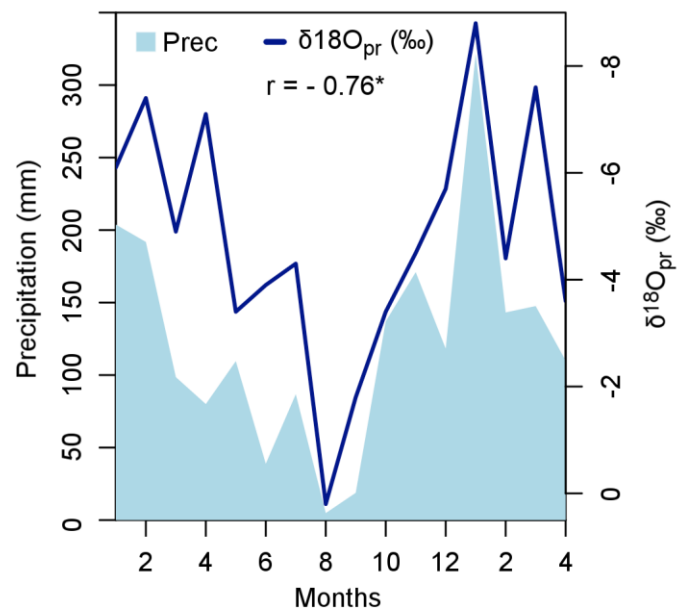
611 *tipu*, and the variable length of the intra-annual samples (distance between vertical

612 black lines) used for the high-resolution stable isotope analyses. For every tree

613 ring, 10 segments had equivalent weight were analyzed.

614

615

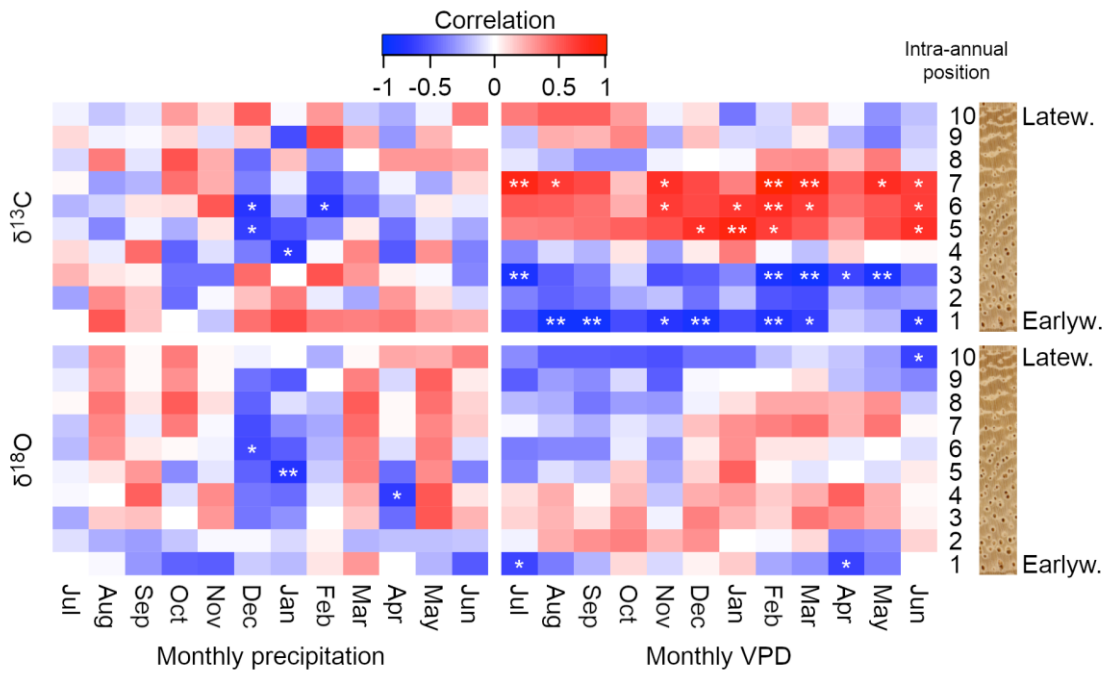


616

617 Figure 3: Oxygen isotope signature of the precipitation ($\delta^{18}\text{O}_{\text{pr}}$) plotted over the
618 monthly precipitation for a period of 16 months (January 2004 to April 2005). *

619 significant for $\alpha = 0.05$.

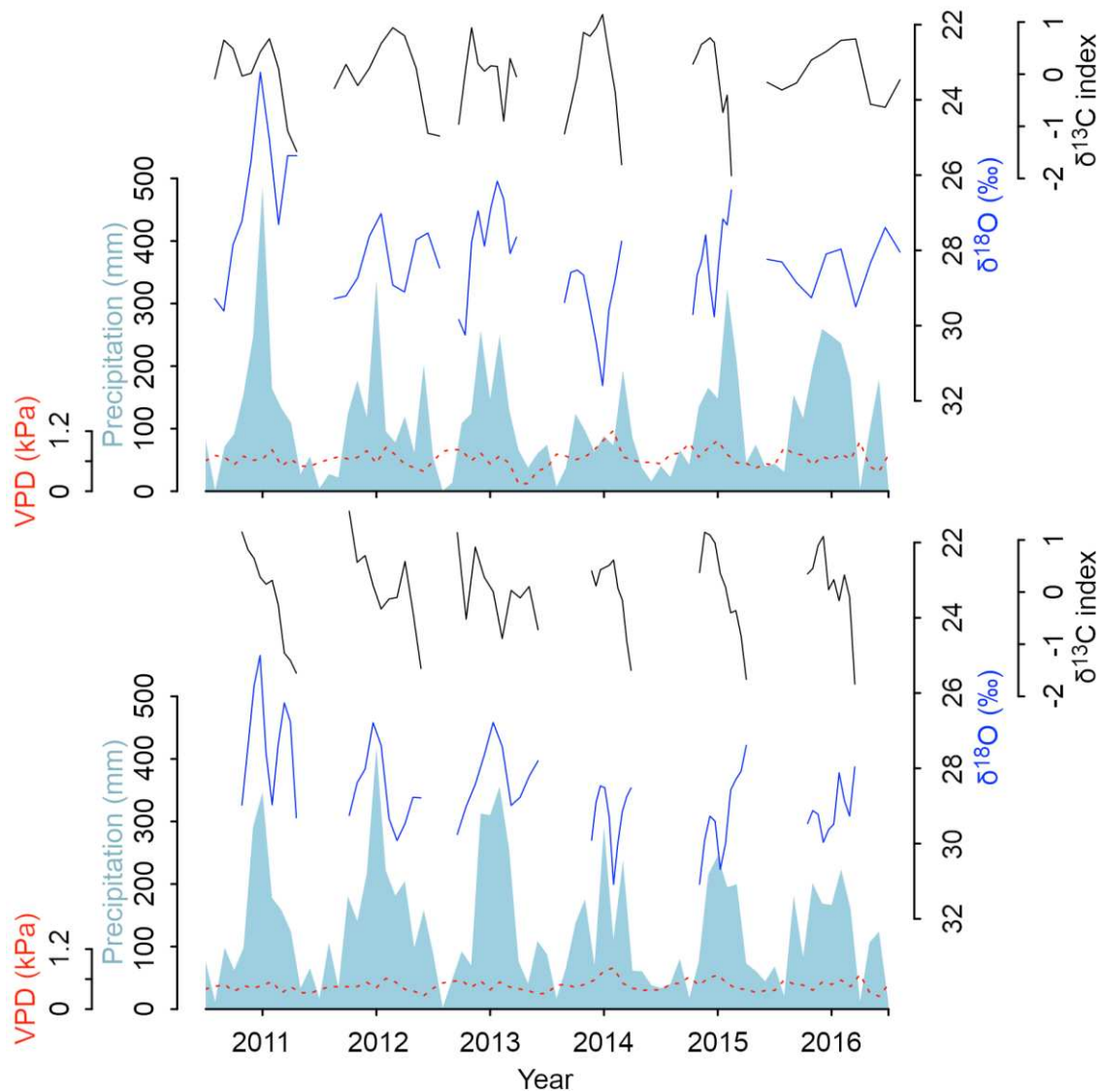
620



621

622 Figure 4: Heatmaps showing the correlation values between oxygen and carbon
 623 stable isotopes from northern and southern populations analyzed together and
 624 monthly precipitation and VPD for the current growing season obtained from
 625 climate stations at the north and south of the Metropolitan Area of São Paulo.
 626 Correlation values are shown by position within the tree ring from earlywood limit
 627 (position 1) to the latewood limit (position 10). * significant values for $\alpha = 0.05$ and
 628 ** for $\alpha = 0.01$.

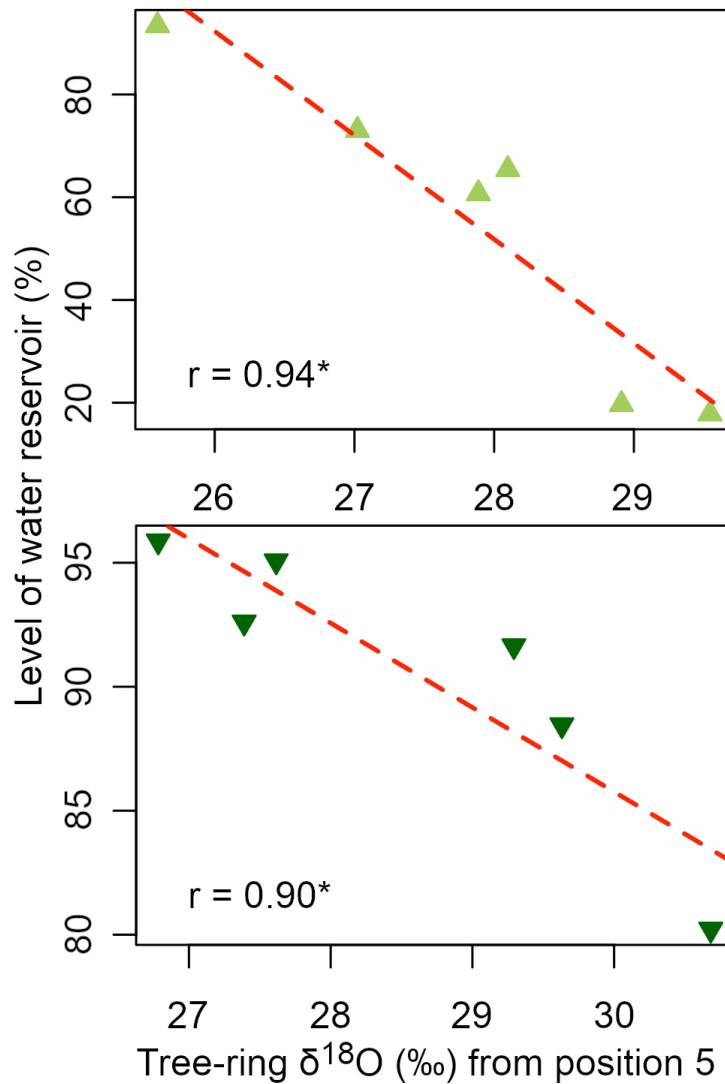
629



631

632 Figure 5: Mean intra-annual stable carbon (here shown as a normalized index) and
 633 oxygen isotopes in the tree rings of *Tipuana tipu* trees and monthly precipitation
 634 and vapor pressure deficit (VPD) from the Northern (upper panel) and Southern
 635 (lower panel) sampling sites in the Metropolitan Region of São Paulo. Series were
 636 aligned with the climate series based on the results of figure 4 (intra-annual tree-
 637 ring position 5 aligned with January).

638



639
 640 Figure 6: Linear relationship (dashed red line) between $\delta^{18}\text{O}$ from position 5 within
 641 the tree ring and the level of the nearest water reservoir in the North (water level
 642 of the Cantareira reservoir system on May, upper panels, $Y = -20 * \delta^{18}\text{O} + 618$)
 643 and South (water level of the Rio Grande reservoir system on February, lower
 644 panels, $Y = -3 * \delta^{18}\text{O} + 188$) of the Metropolitan Area of São Paulo. The respective
 645 correlation coefficients are given for each linear fit, * significant to $\alpha = 0.05$.

646

Table 1: Differences in the mean Gleichläufigkeit (GLK) value calculated for the non-synchronized, and the synchronized intra-annual stable isotopes for the northern and southern populations. Synchronization was based on the $\delta^{18}\text{O}$ series given the assumption of the negative relationship between $\delta^{18}\text{O}$ values of precipitation and its volumes. (Refer to the Figures S4 and S6 to S9 for further details about the synchronization).

Site	$\delta^{18}\text{O}$		$\delta^{13}\text{C}$	
	Non-synchronized	Synchronized	Non-Synchronized	Synchronized
North	0.58	0.82	0.62	0.59
South	0.58	0.70	0.56	0.58

647